

# STUDIES OF LIGHT NUCLEUS CLUSTERING IN RELATIVISTIC MULTIFRAGMENTATION PROCESSES<sup>1</sup>

V.Bradnova<sup>a</sup>, M.M.Chernyavsky<sup>b</sup>, A.Sh.Gaitinov<sup>c</sup>,  
L.A.Goncharova<sup>b</sup>, L.Just<sup>d</sup>, S.P.Kharlamov<sup>b</sup>, A.D.Kovalenko<sup>a</sup>,  
M.Haiduc<sup>e</sup>, V.G.Larionova<sup>b</sup>, F.G.Lepekhin<sup>f</sup>, A.I.Malakhov<sup>a</sup>,  
G.I.Orlova<sup>b</sup>, N.G.Peresadko<sup>b</sup>, N.G.Polukhina<sup>b</sup>,  
P.A.Rukoyatkin<sup>a</sup>, V.V.Rusakova<sup>a</sup>, N.A.Salmanova<sup>b</sup>,  
B.B.Simonov<sup>f</sup>, S.Vokál<sup>d</sup>, P.I.Zarubin<sup>a</sup>, I.G.Zarubina<sup>a</sup>

*a) Joint Institute for Nuclear Research, Dubna, Russia*

*b) P. N. Lebedev Physical Institute, Moscow, Russia*

*c) Institute of Physics and Technology, Almaty, Kazakstan*

*d) P. J. Šafárik University, Košice, Slovakia*

*e) Institute of Space Sciences, Bucharest-Maguerel, Romania*

*f) Petersburg Institute of Nuclear Physics, Gatchina, Russia*

## Abstract

We give an overview of the results and prospects of nuclear clustering studies on the grounds of the observations of interactions of light nuclei with an initial energy above 1·A GeV in nuclear emulsions. Thank to the best spatial resolution and the full solid angle acceptance provided by nuclear emulsions, such an approach allows one to obtain unique and evident observations reflecting cluster-like features in light nuclear structures.

Unique capabilities of emulsion technique are considered as applied to of multifragmentation of peripheral interactions at beam energy of few GeV per nucleon. New results on dissociation of <sup>7</sup>Be and <sup>22</sup>Ne in very peripheral interactions with emulsion nuclei are presented. The importance of this research for the physics of few body nuclear systems and the related problems of nucleosynthesis is noted. The paper is illustrated with characteristic images obtained by means of a microscope equipped with a CCD camera.

The discussed explorations are provided with the beams of the Synchrophasotron and Nuclotron of JINR, Dubna. Future investigations are suggested to be carried out in relativistic beams of He, Be, B, C, and N isotopes.

## 1. Introduction

The BECQUEREL Project (Beryllium (Boron) Clustering Quest in Relativistic Multifragmentation) is oriented toward emulsion expositions by light stable and radioactive nuclei with an energy of the order of few GeV per nucleon in the JINR Nuclotron beams. Observations of the fragmentation of light relativistic nuclei open up new opportunities to explore highly excited nuclear states near multiparticle decay thresholds [1]. Our interest in such states is motivated by their predicted properties as loosely bound systems with spatial spread significantly exceeding the fragment sizes. Natural

---

<sup>1</sup>This work has been supported by the grants 96-15-96423, 03-02-16134, 02-02-164-12a of the Russian foundation of basic researches, of the Slovak Republic and the Slovak Academy of Sciences, and the grants of the JINR Plenipotentiaries of Slovakia, Czechia and Romania for the years 2002 and 2003.

components of such states are the lightest nuclei having no excited states below particle decay thresholds, i. e. deuterons, tritons,  $^3\text{He}$ , and  $^4\text{He}$  nuclei.

A complete spectroscopy of few body decays of highly excited nuclei allows one to search for the Efimov excited states in nuclear systems [2, 3]. The Efimov effect is the remarkable theoretical observation that the number of bound states for three particles interacting via s-wave short range potentials may grow to infinity, as the pair interaction are just about to bind two particles. The Efimov states are loosely bound and their wave functions extend far beyond those of the remaining two particles. Examples of such states in molecular physics are loosely bound helium molecules - dimer  $\text{H}_2$  (of a size about 50 Å), the ground and the first excited state  $\text{H}_3$ . When the three particles are not identical, there are new possibilities for the existence of three-body ground states, like  $^4\text{He}-^4\text{He}-^n\text{H}$  ( $n=1-3$ ) and  $^4\text{He}-^4\text{He}-^3\text{He}$ , He-He-Li, He-He-Na. Since H and He are the most abundant in the universe, these molecules may play a role in the chemistry of the interstellar molecular cloud [4]. Search for analogs of such states on nuclear scale is of undoubted interest since they can play a role of intermediate states ("waiting stations") due to dramatically reduced Coulomb repulsion for nuclear fusions in stellar media.

Other intriguing conjecture is that  $n\alpha$  nuclei near the  $n\alpha$  particle decay threshold can constitute a loosely bound dilute gas forming a Bose condensate [5]. Its major signature is a multiple  $\alpha$  particle decay with a narrowed distribution of relative velocities. Search for such states on the nuclear scale is of undoubted interest since they can play a role of intermediate states ("waiting stations") for a stellar nuclear fusion due to dramatically reduced Coulomb repulsion.

## 2. Research concept

In this respect, a principal experimental task consists in provision of a complete spectroscopy of final fragments - observation of dissociation events, determination of various channel probabilities (branchings), and fragment identification and velocity measurement. Our approach is grounded on spectroscopy of relativistic fragments of incoming nuclei at longitudinal exposures of emulsion layers.

The track detection is performed in emulsion layers measuring  $100\times 200\times 0.5\text{ mm}^3$ . The layers are assembled in few cm thick stacks. The stacks are exposed to a beam in the longitudinal direction. They provide multiple track visualization over the total solid angle with spatial resolution of about 0.5 micron. Their sensitivity extends from slow fragments down to relativistic single charged particles. A mean range of light relativistic nuclei in emulsion is defined by the cross section of their inelastic interaction with emulsion nuclei. It varies from 14 cm for  $^6\text{Li}$  nuclei to 9 cm for  $^{24}\text{Mg}$  in a BR-2 type emulsion. The advantages with respect to low energy researches are the following:

- interactions reach a limiting fragmentation regime above a collision energy of 1A GeV and complex nuclear composition of emulsion doesn't affect isotopic composition of incoming nucleus fragments,
- reactions take the shortest time, especially in cases of electromagnetic and diffractive dissociations,
- projectile nucleus fragments are collimated mostly in a narrow forward cone limited by an angle  $0.2/P_0$ , where  $P_0$  is a primary nucleus momentum; this allows one to obtain 3D image of separated tracks in a single emulsion layer,
- ionization losses of projectile fragments correspond to the minimum and practically don't distort measurements,
- the detection energy threshold for projectile fragments is absent,

- a record spacial resolution of emulsion (0.5 micron) provides a record angular resolution; the excitation scale of a fragmenting system in the projectile rest frame is of the order of few MeV per fragmenting nucleon; in the case of the projectile nucleus fragmentation perfect angular measurements play the determinative role in the estimation of the excitation energy scale while their momentum per nucleon may be taken the same as for an incoming nucleus,
- reliable determination of charges of relativistic fragments is provided over a wide range,
- nuclear clustering manifests itself in the isotope composition of projectile nucleus fragments; via measurement of a total momentum by multiple scattering technique one can identify hydrogen and helium isotopes;
- it is possible to select peripheral interactions corresponding to minimal energy transfers to an incoming nucleus; namely, these events present a major interest for studies of in-flight multiparticle decays.

Visual scanning is concentrated on the events with a total charge transfer of an incoming nucleus to secondary particles in a narrow fragmentation cone. Emulsion nucleus fragmentation and meson production become reduced or even suppressed in this way. Such events amount to a few percent of the total number of inelastic events. In practice, this approach allows one to accumulate statistics of a few tens of peripheral events, which is sufficient for a reliable determination of dominating dissociation channels. Thus, emulsions provide an excellent opportunity of a complete observation and study of light nucleus multifragmentation in flight. The Appendix contains a collection of characteristic images obtained by means of a microscope filming with a CCD camera and reconstructed as flat projections.

For the first time, a coherent multifragmentation was observed and explored in emulsion for  $^{12}\text{C}$  nucleus dissociation into three  $\alpha$  particles at an initial momentum  $4.5\text{A GeV}/c$  [6]-[8]. An example is shown in Fig. 1. The mean free path in emulsions for such events is equal to 5 m, i. e. this study demanded a visual scanning over a long track path to find the statistics of about 100 events. This scale of the statistics is a practical limit of the described approach. Relativistic multifragmentation was also explored for  $^{16}\text{O}$  (examples in Fig. 2 and 3),  $^{24}\text{Mg}$ ,  $^{28}\text{Si}$  nuclei at an initial momentum  $4.5\text{A GeV}/c$  by means of nuclear emulsion [9]-[12] and hydrogen bubble chamber techniques [13]-[15].

Exotic nuclei present a bright extension of nuclear clustering in ground states. The lightest one among them is a  $^6\text{Li}$  nucleus. The important motivation for realizing the above mentioned feasible ways in the investigation of light nuclei became the results of the interactions of relativistic  $^6\text{Li}$  nuclei with emulsion nuclei [17, 18, 19]. We summarize below the results of this investigation basing mostly on the work [18]. They serve to be a prototype of practical tasks for radioactive nuclei suggested in this paper.

At present an analogous analysis of  $^{14}\text{N}$ ,  $^7\text{Li}$  and  $^{11}\text{B}$  exposures is carried out in order to find effects of deuteron and triton clusterings. Our first results for  $^7\text{Be}$  and  $^{22}\text{Ne}$  nuclei are discussed in what follows.

### 3. Clustering in $^6\text{Li}$ nucleus

A stack formed by emulsion layers was exposed to a beam of  $4.5\text{A GeV}/c$   $^6\text{Li}$  nuclei at the Synchrotron. During irradiation, the beam was directed in parallel to the emulsion plane. The first intriguing feature is that the mean free path of  $^6\text{Li}$  nuclei was found to be strongly decreased as compared with the expected value. The obtained value would correspond to a nucleus with mass number  $A$  equal to 11. This points to

an unusually large radius of the nucleon distribution in  ${}^6\text{Li}$  nucleus. Using the geometric overlapping model, its value was estimated to be  $2.7\pm 0.1$  fm, which is in a reasonable agreement with the known data on elastic scattering of protons on a  ${}^6\text{Li}$  target.

Another distinctive feature of the  ${}^6\text{Li}$  nucleus was got by means of a multiple track scattering analysis, which allowed one to establish the isotopic composition of relativistic fragments. An unusually enhanced yield of relativistic deuterons was established to be the same as the proton one. A subsequent analysis dealt with  ${}^3\text{He}$  and  ${}^4\text{He}$  nuclei. The fragmentation of  ${}^6\text{Li}$  in the form of clusters consisting of  ${}^3\text{He}$  and tritium nuclei was shown to be by an order of magnitude weaker than the structure produced by an  $\alpha$  particle and a deuteron. This explains an increased yield of deuterons as a reflection of the structure of weakly bound clusters of the  $\alpha$  particle and the deuteron.

The fragmentation channel  ${}^6\text{Li}$  points to a lower value of the mean transverse momentum of  $\alpha$  particles,  $\langle P_T \rangle = 0.13 \pm 0.1$  GeV/c when compared with the case  ${}^{12}\text{C}$  having  $\langle P_T \rangle = 0.24 \pm 0.01$  GeV/c. In the spirit of an uncertainty relation, this fact is another indication to an increased size of  ${}^6\text{Li}$  nucleus.

Among the 1000 found  ${}^6\text{Li}$  interactions it is possible to consider as "golden" 31 events of coherent  ${}^6\text{Li}$  dissociation not accompanied by the target nucleus excitation ("white stars"). An example is shown in Fig.4. Among them 23 events correspond to the dissociation channel  $\alpha+d$ , four of them to  ${}^3\text{He}+t$ , four to  $t+d+p$  and none of them to  $d+d+d$ . This topology shows the cluster structure of  ${}^6\text{Li}$  nucleus in the most obvious manner. Thanks to the completely reconstructed coherent dissociation kinematics it became possible to reconstruct the  ${}^6\text{Li}$  levels at 2.19 and 4.31 MeV with isotopic spin  $T=0$ . On the contrary, the 3.56 MeV level with isotopic spin  $T=1$  is absent because of the  $\alpha+d$  system isotopic spin  $T=0$ . This is the very clear illustration of an isotopic filtering in strong interactions.

#### 4. Clustering in ${}^{10}\text{B}$ dissociation

${}^{10}\text{B}$  nuclei were accelerated at the JINR Nuclotron, and a  ${}^{10}\text{B}$  nucleus beam of energy of 1A GeV was formed. The beam was used to irradiate stacks composed of BR-2 type emulsion layers. During irradiation, the emulsion layers were located in parallel to the beam direction so that the beam particles could enter the butt-end of the emulsion layers. Search for nucleus-nucleus interactions was performed by visual scanning of particle tracks by means of microscopes ( $\times 900$  magnification). At a scanned track length of 138.1 m, it was found 960 inelastic interactions of  ${}^{10}\text{B}$  nuclei. The mean free path of  ${}^{10}\text{B}$  nuclei to an inelastic interaction in emulsion was found to be  $14.4 \pm 0.5$  cm. This value meets well the dependence of the mean free path upon the atomic number of a bombarding nucleus for light nuclei having homogeneous nucleonic density.

Information about the charge composition of charged fragments and about the channels of  ${}^{10}\text{B}$  nucleus fragmentation in peripheral collisions has been obtained. We attribute to the peripheral interactions events in which the total charge of relativistic fragments is equal to the charge of the primary  ${}^{10}\text{B}$  nucleus, the production of charged mesons is not observed, while the production of slow nuclear fragments is allowed in selection. In order to single out such events by visual observation we estimated the charges of relativistic particles and the total charge of relativistic particles with emission angles less than  $15^\circ$  with respect to the  ${}^{10}\text{B}$  direction. For the primary beam energy of 1A GeV, this value corresponds to the proton transverse momentum of 0.44 GeV/c. Then using measuring microscopes we evaluated the emission angles of all particles in the selected events. The particle charges were determined by the length of spacings in their tracks.

The number of the found events in which the total charge of fragments is equal to five and in which charged mesons are not observed is equal to 93 (10% of all the events). We notice that the selection of events in which the production of even nuclear

emulsion fragments is forbidden decreases statistics down to 41 events ("white stars"). In this case, the distribution of statistics by channels remains practically unchanged.

In 65% of such peripheral interactions the  $^{10}\text{B}$  nucleus is disintegrated to two double charged and a one single-charged particles (Fig. 5). A single-charged particle is the deuteron in 40% of these events. 10% of events contain fragments with a charge equal to 3 and 2 (Li and He isotopes), and 2% of events contain a fragment with charges equal to 4 and 1 (Be nucleus and the proton). The  $^6\text{Li}$  production accompanied by an alpha particle may be considered as a correlation of  $\alpha$  particle and deuteron clusters. Fig. 6 shows an example of a two-particle decay to Li and He fragments. The fragmentation channel containing  $\alpha$  particle and three single-charged fragments (disintegration of one of the  $\alpha$  clusters) makes up 15%. An equal correlation of the channels  $(\text{He}+\text{He}+\text{d})/(\text{He}+\text{He}+\text{p})\approx 1$  is analogous to the  $^{10}\text{Li}$  fragmentation where  $(\text{He}+\text{d})/(\text{He}+\text{p})\approx 1$ . These ratios point to an abundant yield of deuterons in the  $^{10}\text{B}$  case too [18, 19].

Thus, the deuteron cluster manifests itself directly in the three-particle decays of  $^{10}\text{B}$  nuclei accompanied by two two-charged particles. Another indication to deuteron clustering is a small mean transverse momentum of deuterons  $P_T=0.14\pm 0.01$  GeV/c in these events, in just the same way as in the case of  $^6\text{Li}$ , where  $P_T=0.13\pm 0.02$  GeV/c.

We note that  $^{10}\text{B}$  nucleus, like the deuteron, and  $^6\text{Li}$  and  $^{14}\text{N}$  belong to a rare class of even-even stable nuclei. Therefore, it is interesting to establish the presence of deuteron clustering in relativistic  $^{14}\text{N}$  fragmentation as well as the appearance of  $^8\text{Be}$  clustering (example in Fig. 7).

### 5. Clustering in $^7\text{Li}$ dissociation

A total of 1274 inelastic interactions were found to be occurred in a nuclear emulsion irradiated by a  $^7\text{Li}$  beam with a momentum  $3A$  GeV/c at the JINR Synchrophasotron, at a length of 185 m of scanned tracks. The mean free path of  $^7\text{Li}$  nuclei up to an inelastic interaction in emulsion was found to be  $14.5\pm 0.4$  cm which coincides, within errors, with the  $^7\text{Li}$  mean free path [17, 18, 19]. The close values of the mean free paths and the total transverse cross sections of inelastic interactions of  $^6\text{Li}$  and  $^7\text{Li}$  point out that their effective interaction radii are also close in magnitude to each other.

About 7% of all inelastic interactions of  $^7\text{Li}$  nuclei are peripheral interactions (80 events), which contain only the charged fragments of a relativistic nucleus, they do not contain any other secondary charged particles, and the total charge of the fragments is equal to the charge of a fragmenting nucleus ("white stars"). All these events are actually two-particle  $^7\text{Li}$  decays to one double and one single-charged fragments. Half of these events are attributed to a decay of  $^7\text{Li}$  nucleus to an  $\alpha$  particle and a triton (40 events). The number of decays accompanied by deuterons makes up 30%, and by protons - 20%.

The isotopic composition of decayed particles points to the fact that these events are related to the structure as the  $\alpha$  particle and triton clusters. The predominance of tritons in the isotopic compound of single-charged fragments shows well the dominating role of the triton cluster in the  $^7\text{Li}$  fragmentation in very peripheral interactions with emulsion nuclei.

Similar two-particle  $^6\text{Li}$  decays to an  $\alpha$  particle and a deuteron which reflected the weakly bound two-cluster nuclear structure were registered in inelastic peripheral interactions of  $^7\text{Li}$  nuclei with a momentum  $4.5A$  GeV/c in emulsion. Thus, the structure in the form of the  $\alpha$  particle core and external nucleons bound into a cluster is typical not only of  $^6\text{Li}$  nucleus, but also of  $^7\text{Li}$  one. The obtained value of the cross section for coherent decay to an  $\alpha$  particle and a triton,  $27\pm 4$  mb, was found to be about the same as the cross section of paper [18] for  $^6\text{Li}$  decay to  $\alpha$  particle and a deuteron

22±4 mb. This may be viewed as an indication to the fact that the mechanisms of the decays in question are of the same nature. It is interesting to continue to clear up a possible role played by the tritons as cluster elements in  $^{11}\text{B}$  and then in  $^{15}\text{N}$  nuclei.

## 6. Clustering in $^6\text{He}$ dissociation

Using a  $^6\text{Li}$  nucleus beam extracted from the JINR Synchrophasotron at momentum 2.67A GeV/c a secondary beam was produced with a composition of 1% of  $^6\text{He}$  and 99% of  $^3\text{H}$  nuclei [20].

The major feature of  $^6\text{He}$  nucleus interactions with nuclei is due to a peculiar interaction of an external neutron pair with the target nucleus. The process  $^6\text{He} \rightarrow \alpha + n + n$  is possible in a peripheral interaction in which a break-up of external neutrons occurs without a secondary particle production ("white stars"). An example is shown in Fig. 8. The determination of the process probability and measurement of the angular distribution of produced  $\alpha$  particles is one of the major tasks of  $^6\text{He}$  nucleus experimental studies. Such events are presented in emulsion by an image of a scattered track of a double charged particle. Analogous  $^6\text{Li}$  nucleus interactions in emulsion with  $\alpha$  particles in the final state were observed due to reactions  $^6\text{Li} \rightarrow \alpha + d$  and  $^6\text{Li} \rightarrow \alpha + p + n$  in [18].

Indeed, in this study, on a 457 cm scanned path of double charged tracks it was found 23 inelastic interactions having secondary particles and, in addition, 5 events of a gradual change of the direction behind a scattering point. The mean momentum in these five events is equal to  $15.6 \pm 3.8$  GeV/c, and after scattering to  $9.1 \pm 2.6$  GeV/c. The scattering angle do not exceed  $0.35^\circ$  in all the found cases, and the mean transverse momentum of  $\alpha$  particles  $\langle P_T \rangle$  is about 0.035 GeV/c. We notice that in dissociation processes  $^6\text{Li} \rightarrow \alpha + d$  and  $^6\text{Li} \rightarrow \alpha + p + n$  at a  $^6\text{Li}$  nucleus momentum 4.5A GeV/c the corresponding  $\langle P_T \rangle$  is about 0.15 GeV/c [17, 18, 19].

A narrower transverse momentum distribution in the process points to a very peripheral picture of  $\alpha$  particle production in a coherent interaction. A mean free range defined on the 457 cm path taking into account the registered coherent interactions is  $16.3 \pm 3.1$  cm. This value is larger than the corresponding one for a  $^6\text{Li}$  nucleus determined in [17, 18, 19] as  $14.3 \pm 0.3$  cm. It might be assumed that the excessive value can be explained by an assumption of a 50% identification efficiency of the process. The validity of such an assumption will indicate that the contribution of coherent interactions to the total cross-section exceeds 20%

## 7. Clustering in $^7\text{Be}$ dissociation

Advantages of emulsion technique are exploited most completely in the study of peripheral fragmentation of light stable and neutron deficient nuclei. A secondary beam containing a significant fraction of 1.23A GeV  $^7\text{Be}$  nuclei was formed at the JINR Nuclotron by selecting the products of charge exchange of primary  $^7\text{Li}$  nuclei with the aid a beam transport channel. Emulsion stacks have been irradiated. The  $^7\text{Be}$  nucleus is convenient for magnet optics selection due to the maximum ratio of the charge to the weight. Besides, it gives the most complete observation of final fragments.

By visual scanning along tracks, we have found 22 decays of incoming nuclei to helium fragments without other accompanying tracks ("white stars"). The event examples are shown in Fig. 9. Helium isotopes have been identified via their total momenta derived from multiple scattering measurements. This makes it possible to conclude, that a dominant fraction is due to a coherent dissociation  $^3\text{He} + ^4\text{He}$  and only 2-3 decays to  $^3\text{He} + ^3\text{He} + n$ . We have found 20 events with charged topology of relativistic fragments 2+1+1 ("white stars") with identified  $^3\text{He}$  and 16 with identified  $^4\text{He}$ . The events with topology 3+1 and 1+1+1+1 are presently analysed. They represent only a few percent fraction.

Thus, one can conclude that a  $^3\text{He}$  clustering manifests in decays of excited relativis-

tic  ${}^7\text{Be}$  nuclei. This result agrees with our expectations. It seems to be useful for future studies of the role of  ${}^3\text{He}$  clusterization in three body decays of  ${}^8\text{B}$  ( ${}^1,2\text{H}-{}^4,3\text{He}-{}^3\text{He}$ ),  ${}^9\text{C}$  ( ${}^3\text{He}-{}^3\text{He}-{}^3\text{He}$ ),  ${}^{10}\text{C}$  ( ${}^3\text{He}-{}^3\text{He}-{}^4\text{He}$ ), and  ${}^{11}\text{C}$  ( ${}^3\text{He}-{}^4\text{He}-{}^4\text{He}$ ). It is quite possible that  ${}^3\text{He}$  clustering could play a role analogous to the role of a triple  $\alpha$  process in stellar nucleosynthesis.

### 8. Clustering in ${}^{22}\text{Ne}$ dissociation

We reanalyzed of existing data (DST) on about 4100  ${}^{22}\text{Ne}$  4.1A GeV/c interactions in an emulsion. We found 94 events containing only fragments of a primary nucleus without target nucleus fragments and produced mesons ("white stars").

The dominant channel is 8+2 – 53 events (He cluster separation), the follow 9 + 1 – 14, 7 + 2 + 1 – 7, 8 + 1 + 1 – 6, 6 + 2 + 2 – 5, 6 + 2 + 1 + 1 – 3. Among deeper fragmentation there are 2 events 4+1+1+1+1+1+1 and 4 + 2 + 2 + 2, and single events with topologies 5 + 2 + 1+ 1+ 1, 5 + 2 + 2 + 1, 3 + 2 + 1 + 1 + 1 + 1 + 1, and 2 + 2 + 2 + 2 + 1 + 1. The most interesting fact is that we have found 3 events of topology 2+2+2+2+2, corresponding neon dissociation into helium nucleus fragments only. The example is shown in the Fig. 10.

In our opinion, such distribution of final charged states brightly illustrate transition from a single helium fragment splitting to a total multifragmentation of the explored nucleus. Absence in the selected statistics of binary fissions like 7+3, 6+4, 5+5 is especially interesting. We plan to carry out a detailed kinematical analysis of these events.

Universality of a coherent dissociation mechanism enables us to search for such events in emulsions irradiated by  ${}^{24}\text{Mg}$ ,  ${}^{28}\text{Si}$ , and  ${}^{32}\text{S}$  nuclei at 4.5A GeV/c in order to study a relative role of multiparticle decays. Examples of  ${}^{24}\text{Mg}$  peripheral interactions with growing dissosiation degree are shown in the Fig. 11-15.

Verification of a hypothesis about the phase transition of light nuclei from a ground state to multiparticle one via a Bose condensate is one of intriguing perspectives of this research.

### Acknowledgements

The development of our project would not have been possible without scientific guidance and support of late Academician A. M. Baldin. We are indebted to late Prof. M. I. Adamovich for many year leadership in emulsion technique. Papers of late Prof. G. M. Chernov on nuclear coherent dissociation has played inspiring role in our research. Our manuscript is devoted to the memory of these outstanding scientists.

The authors express their warmest thanks to A. V. Pisetskaya from FIAN, Moscow and I. I. Sosulnikova, A. M. Sosulnikova, N. A. Kachalova, G. V. Stelmakh, and A. Vokálova from JINR, Dubna for their contribution in a microscope visual analysis and I. I. Marin for perfect maintenance of microscopes. Emulsion proceeding was performed by the LHE JINR chemist group with excellent quality.

Valuable contributions to our work have been provided by the JINR Synchrophasotron and Nuclotron personnel and the beam transport group.

## References

- [1] V. Bradnova et al. Few-Body Systems Suppl. 14 (2003) 241.
- [2] V. Efimov Phys. Lett. B33, 563 (1970).
- [3] F. Nunes C. R. Physique 4 (2003) 489-485.

- [4] Yong Li and C D Lin J. Phys. B: At. Mol. Opt. 32(1999)4877-4883.
- [5] P. Schuck, H. Horiuchi, G. Ropke, A. Tohsaki, C. R. Physique 4 (2003) 537-540.
- [6] V. V. Belaga et al.: Phys.Atom.Nucl. **58**, 1905 (1995)
- [7] V. V. Belaga et al.: Phys.Atom.Nucl. **60**, 791 (1997)
- [8] V. V. Belaga, M. M. Muminov, G. M. Chernov: JETP Letters **62**, 395.
- [9] N. P. Andreeva et al.: Phys. Atom. Nucl. **59**, 102 (1996)
- [10] M. A. Belov et al.: Phys. Atom. Nucl. **65**, 959 (2002)
- [11] M. L. Allaberdin et al.: e-Print Archive: nucl-ex/0102006
- [12] A. I. Bondarenko et al.: Sov. J. Nucl. Phys. **55**, 77 (1992)
- [13] V. V. Glagolev et al.: Eur. Phys. J. **A11**, 285 (2001)
- [14] V. V. Glagolev et al.: Phys. Atom. Nucl. **63**, 520 (2000)
- [15] V. V. Glagolev et al.: Phys. Atom. Nucl. **62**, 1388 (1999)
- [16] V. G. Bogdanov et al.: JETP Lett. **44**, 391 (1986)
- [17] M. El-Nadi et al.: In: Proceedings of International School of Cosmic Ray Astrophysics, 10th Course, Erice (1996).
- [18] M. I. Adamovich et al. Phys. At. Nucl., vol. 62, N8, 1999, pp 1378-1387.
- [19] F. G. Lepekhin, D. M. Seliverstov, B. B. Simonov. Eur. Phys. J. A, 1, 137-141 (1998).
- [20] M. I. Adamovich et al.: Part. and Nucl., Letters., **N1[110]**, 29 (2002); e-Print Archive: nucl-ex/0206013.

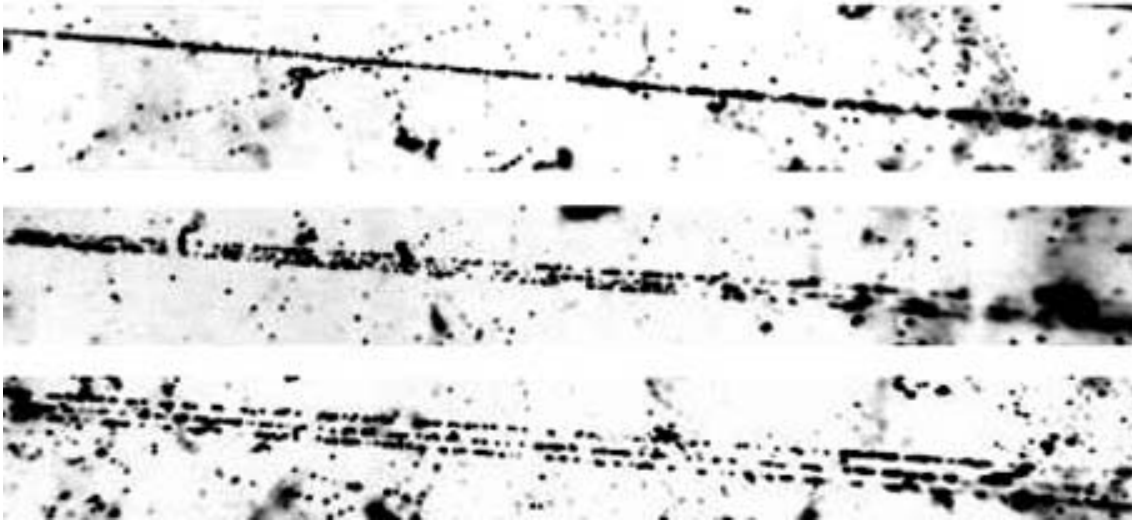


Figure 1: Event of dissociation of a  $4.5A \text{ GeV}/c$   $^{12}\text{C}$  nucleus in peripheral interaction into three  $\alpha$  particles shown in subsequent evaluation. Upper photo: interaction vertex with production of a narrow fragment jet. Middle and lower photo: shifting from vertex allow one to identify three double charged fragments.



Figure 2: Event of asymmetric binary splitting of a  $4.5A \text{ GeV}/c$   $^{16}\text{O}$  nucleus in peripheral interaction. Upper photo: interaction vertex with production of narrow fragment jet. Lower photo: shifting from vertex allows one to resolve relativistic C and He fragments.

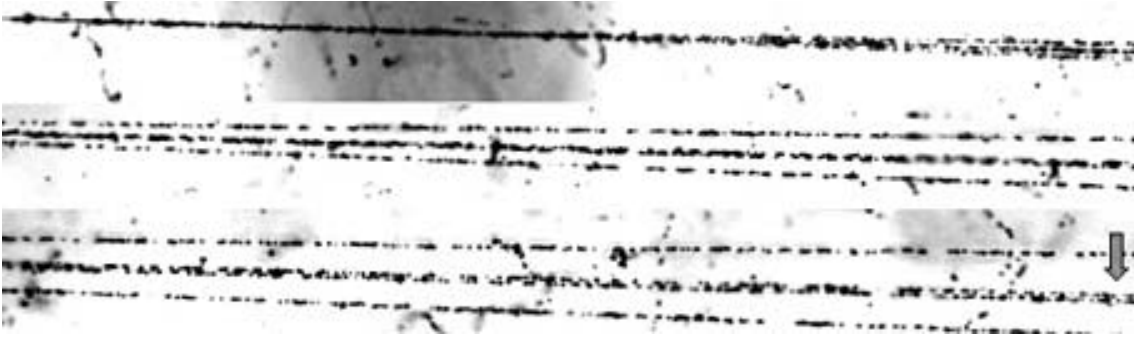


Figure 3: Event of dissociation of a  $4.5A$  GeV/c  $^{16}\text{O}$  nucleus in peripheral interaction into four He fragments. Upper photo: interaction vertex with production of a narrow fragment jet. Middle photo: shifting from vertex allow one to identify two He fragments and a very close track pair. Lower photo: further shifting allows one to resolve the central pair on the previous photo as a relativistic  $^8\text{Be}$  production.

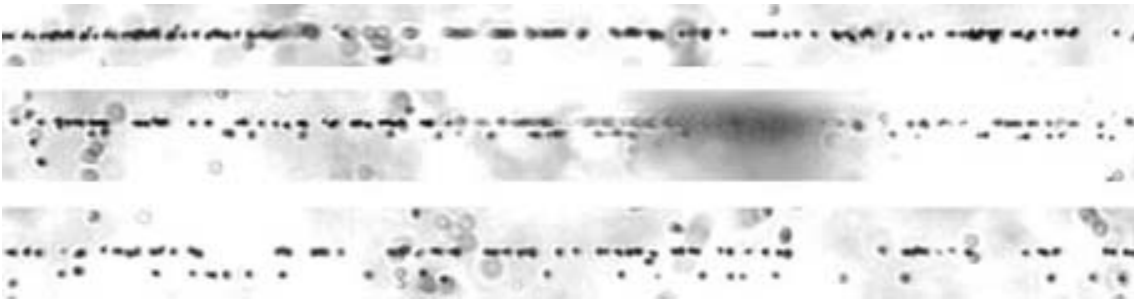


Figure 4: Event of dissociation of a  $4.5A$  GeV/c  $^6\text{Li}$  nucleus in peripheral interaction into H and He fragments. Upper photo: interaction vertex with production of a very narrow fragment pair. Lower photo: shifting from vertex allow one to resolve double and single charged relativistic fragments.

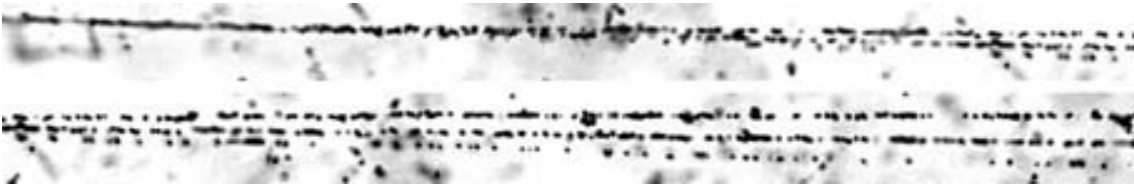


Figure 5: Event of dissociation of a  $1A$  GeV  $^{10}\text{B}$  nucleus into two double and one single charged fragments.

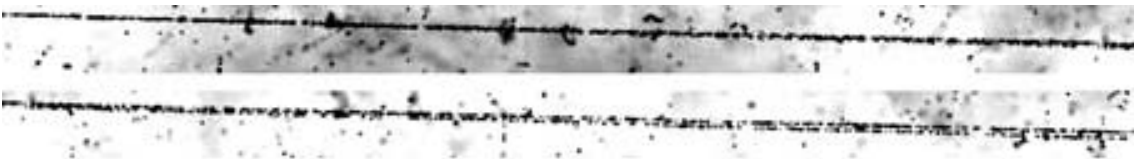


Figure 6: Event of a  $1A$  GeV  $^{10}\text{B}$  nucleus dissociation to a Li (top) and He fragments (bottom).

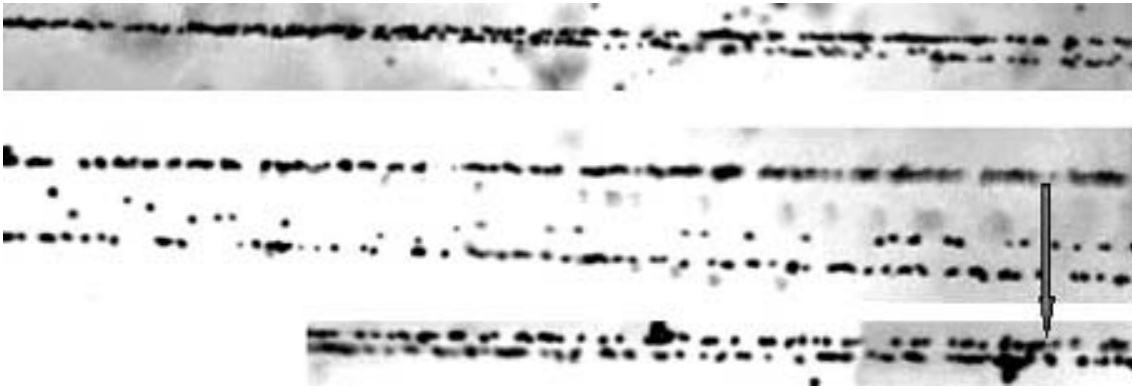


Figure 7: Event of dissociation of a  $4.5A$  GeV/c  $^{14}\text{N}$  nucleus in peripheral interaction into three He and one H fragments. Upper photo: interaction vertex with production of a narrow fragment jet. Middle photo: shifting from vertex allows one to identify single H and He relativistic fragments accompanied by a very close track pair (top). Lower photo: further shifting allows one to resolve the central pair on the previous photo as a relativistic  $^8\text{Be}$  production.

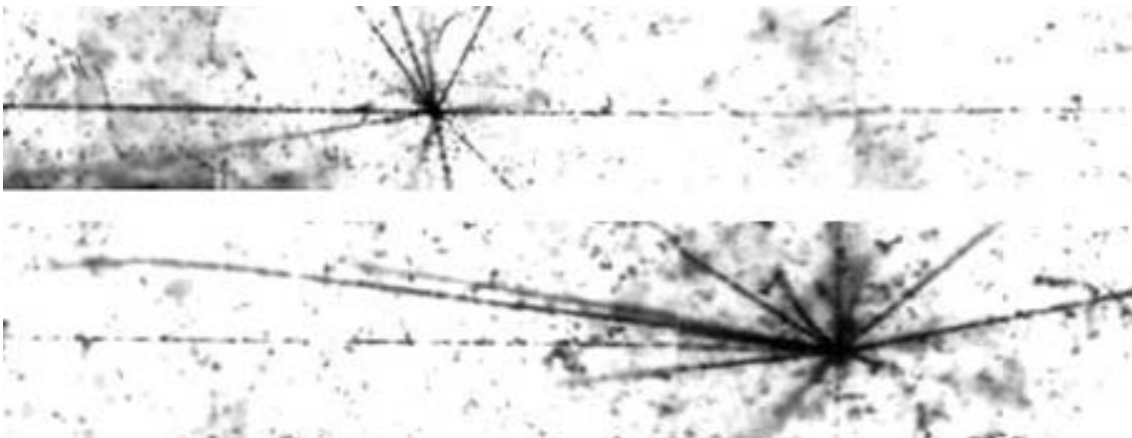


Figure 8: Event of a  $2.67A$  GeV  $^6\text{He}$  nucleus interaction with fragmentation into a relativistic  $\alpha$  particle. The  $\alpha$  particle track is followed until a violent inelastic interaction.

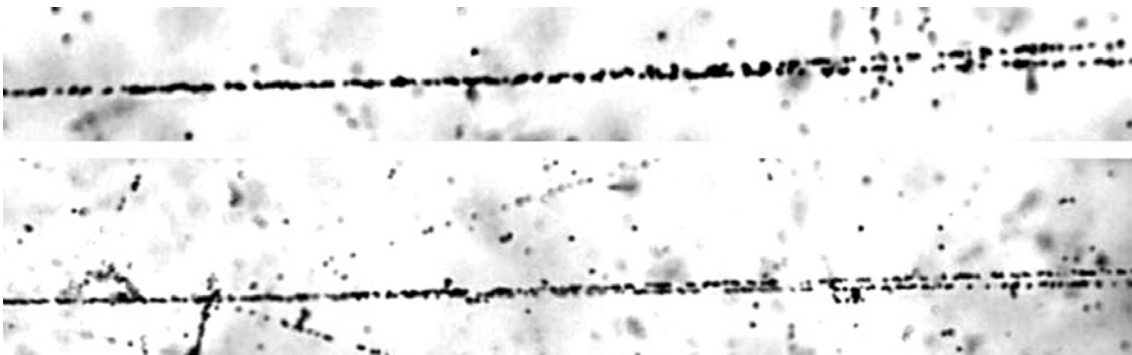


Figure 9: Examples of peripheral dissociation of  $1.23A$  GeV  $^7\text{Be}$  nuclei into pairs of He nuclei. Upper photo: dissociation without target nucleus excitation and produced charged mesons. Lower photo: dissociation accompanied by a target fragment and a meson like pair.

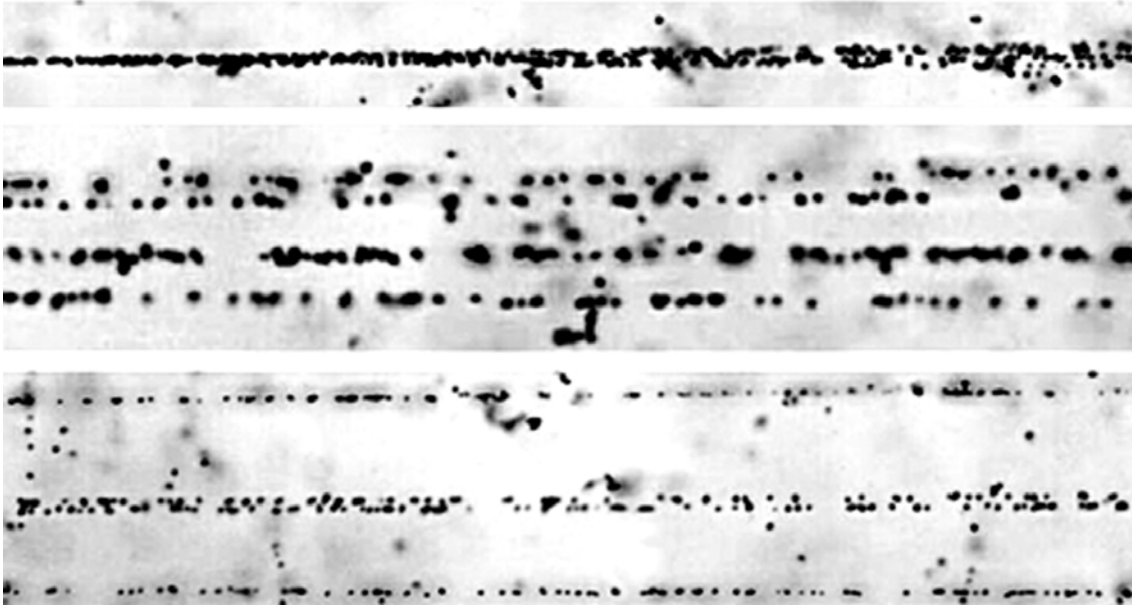


Figure 10: Dissociation of a  $4.5A$  GeV/c  $^{20}\text{Ne}$  nucleus in peripheral interaction into five He fragments. Upper photo: Interaction vertex with production of a narrow fragment jet. Middle photo: shifting from vertex allows one to identify three He fragments. Lower photo: further shifting allows one to resolve a central track on the previous photo as a very narrow pair of relativistic He nuclei ( $^8\text{Be}$  production).

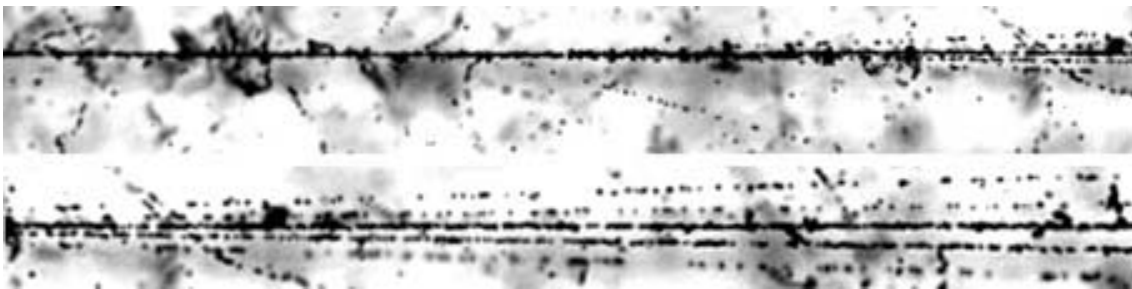


Figure 11: Event of dissociation of  $4.5A$  GeV/c  $^{24}\text{Mg}$  nucleus in peripheral interaction into charged topology  $1+1+7+2+1$  (from top to bottom). Upper photo: interaction vertex with production of narrow fragment jet accompanied with a relativistic meson like track. Lower photo: shifting from vertex allows one to resolve five fragments.



Figure 12: Event of dissociation of a  $4.5A \text{ GeV}/c$   $^{24}\text{Mg}$  nucleus in peripheral interaction into charged topology  $1+1+2+2+1+5$  (from top to bottom). Upper photo: interaction vertex with production of a narrow fragment jet accompanied with a relativistic meson like track. Lower photo: shifting from vertex allows one to resolve six relativistic fragments.

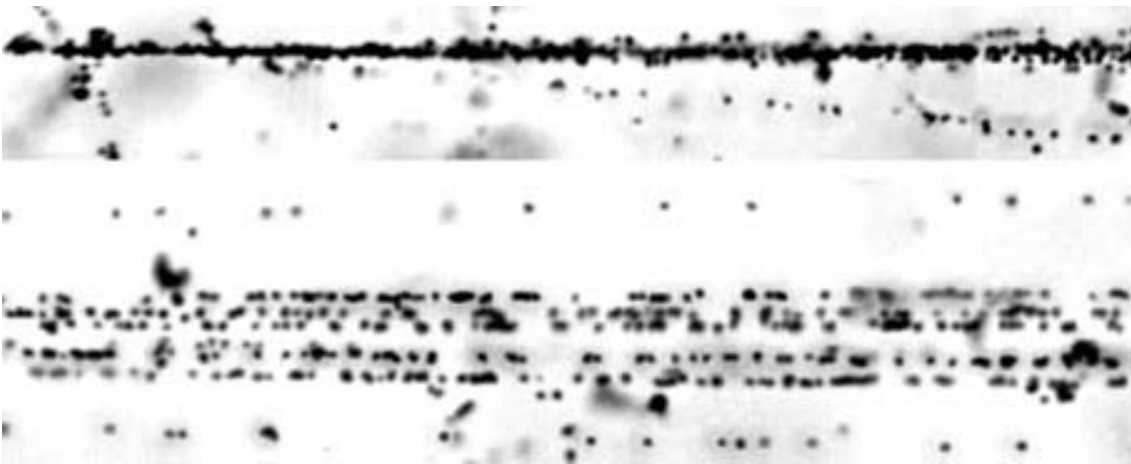


Figure 13: Event of a  $4.5A \text{ GeV}/c$   $^{24}\text{Mg}$  nucleus dissociation into five double and two single charged fragments. Upper photo: interaction vertex with production of narrow fragment jet accompanied with a relativistic meson like track. Lower photo: shifting from vertex allows one to resolve seven relativistic fragments.

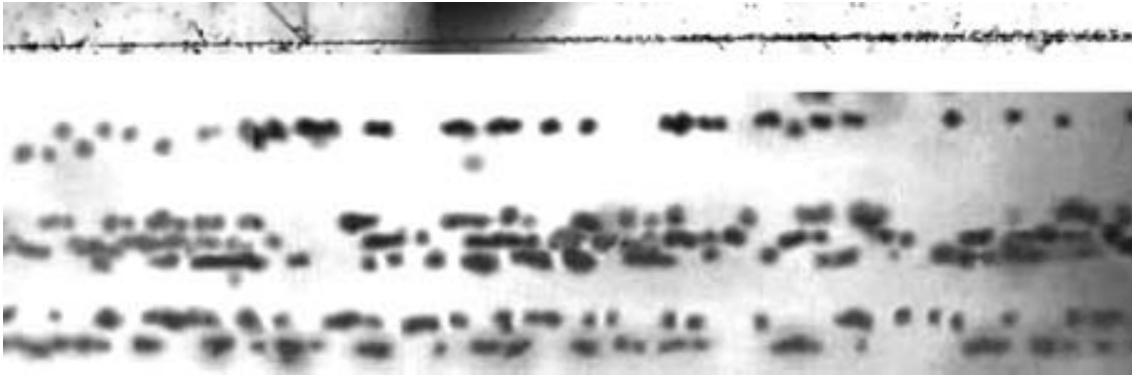


Figure 14: Event of dissociation of a  $4.5A$   $\text{GeV}/c$   $^{24}\text{Mg}$  nucleus in peripheral interaction into six He fragments. Upper photo: interaction vertex with production of a narrow fragment jet accompanied with a couple of target slow fragments. Lower photo: further shifting allows one to resolve (from top to bottom) separate He fragment, very narrow He fragment triple (most probably, decay of excited  $^{12}\text{C}$  nucleus), and a very narrow He pair ( $^8\text{Be}$  production).

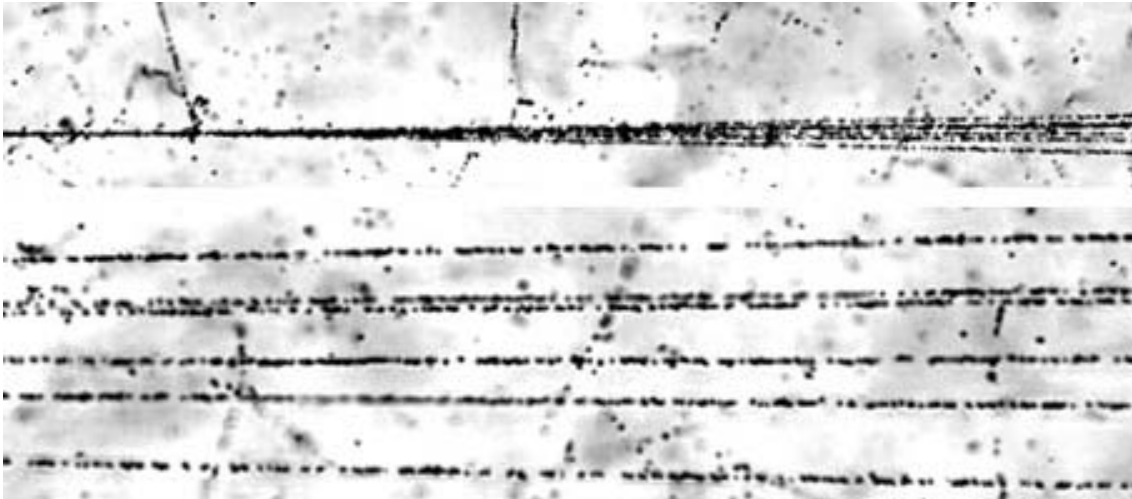


Figure 15: Event of dissociation of a  $4.5A$   $\text{GeV}/c$   $^{24}\text{Mg}$  nucleus in peripheral interaction into five  $\alpha$  particles and single  $^3\text{He}$  fragments. Upper photo: interaction vertex with production of narrow fragment jet accompanied with a target recoil. Lower photo: further shifting allows one to resolve (from top to bottom) a six He fragment system containing a very narrow  $\alpha$  particle pair ( $^8\text{Be}$  production).